Test of the equipartition principle for granular spheres in a saw-tooth shaker

1996 J. Phys. A: Math. Gen. 29 4365

(http://iopscience.iop.org/0305-4470/29/15/011)

J. Phys. A: Math. Gen. **29** (1996) 4365–4386. Printed in the UK

Test of the equipartition principle for granular spheres in a saw-tooth shaker

Trevor A Knight and Leslie V Woodcock

Department of Chemical Engineering, University of Bradford, Bradford BD7 1DP, UK

Received 3 August 1995, in final form 26 January 1996

Abstract. The equipartition-of-energy principle has been tested for a simple model system of weightless granular media comprising inelastic spheres being shaken at a steady state in a uniaxially vibrating box. Granular dynamics simulations are reported and compared with a theoretical model based on the axioms of classical kinetic theory. For inelastic particles, both frictionless and with rotational degrees of freedom, the shaker reaches a steady state. Both the theoretical model and the simulation results show that equipartition always prevails at sufficiently small vibration amplitudes, irrespective of the frequency, over the whole density range. The independence of the reduced energy on frequency is an exact scaling result. When the shaker amplitude increases to the same order as a density-dependent characteristic path length, there are significant deviations from equipartition behaviour. In all the simulations, a Maxwell–Boltzmann distribution of velocities closely prevails within each degree of freedom, even when equipartition is not obtained between the longitudinal and transverse directions. The steady-state energetics of the saw-tooth shaker are evaluated analytically by means of an energy balance using exact kinetic theory and the known hard-sphere fluid collision frequency via the equation of state. This gives rise to scaling laws which enable granular-'thermodynamic' and transport properties of the fluidized granular material to be determined from the corresponding-state thermodynamic and transport properties of the classical hard-sphere fluid in thermal equilibrium.

1. Introduction

In recent years there have been numerous attempts to extend the concepts of classical thermodynamics to granular materials. Of particular interest recently are the theoretical studies of Edwards and co-workers (1993) in which the role of 'entropy' in the specification of a powder is considered from a statistical mechanical viewpoint. Whilst the statistical mechanical entropy for a static powder may be a useful concept, ground-state 'entropy' is analogous to the zero-point thermodynamic state function. As such, its application to the state of a granular solid requires a formal macroscopic definition by analogy with classical thermodynamics. The fundamental question then arises: to what extent can the state of a dynamic granular material be characterized by quasi-thermodynamic state functions such as granular 'temperature' or granular 'entropy'?

The simplest treatable model of a powder is a collection of classical, monodisperse, frictionless dynamical spheres, which are continuously or systematically densified by a well defined densification process until they are so dense that they are in a quasi-vitreous state. If the hard-sphere glass (amorphous solid) is produced via such stable and metastable path states of the thermal hard-sphere fluid, classical thermodynamic formulae can be used to define and calculate the residual entropies, volumes and other excess properties relative to the crystalline state, of the hard-sphere model glass (Woodcock 1981).

0305-4470/96/154365+22$19.50

Alternatively, all granular materials at rest could be regarded as colloidal glasses; many common transport and mixing processes involve the fluidization of these materials. In these processes the particles acquire kinetic energy which can be transferred from one particle to another in collisions, just like molecules. It therefore seems worthwhile to ask whether, under steady-state conditions, when mechanical energy of shaking is continuously being converted to heat by inelastic collisions, the principle thermodynamic condition of 'equipartition of energy' can prevail. If so, under what conditions does 'granular thermodynamics' exist as a *bone fide* subject? An answer to this question, for any well defined process, if affirmative, might not only lend authenticity to the concept of 'entropy' or 'free energy' of granular materials, eventually, but it could provide the 'reversible paths' that will enable such properties to be calculated by computer simulations. Particulate computer simulations are now becoming an indispensable tool for obtaining insights into many aspects of fluidized granular media; the general computational approach has been reviewed recently by Barker (1993).

Ingenious experimental studies on vibrating bead systems, involving high-speed photography, have also been reported recently (Warr *et al* 1995a). These studies enable the velocity distributions to be observed experimentally; preliminary results for two-dimensional systems indicate complex and subtle deviations from Maxwell distributions when a gravitational field acts in the same direction as the vibration. Computer simulation, however, may be better placed to investigate these phenomena for very simple models in the absence of gravity. The purpose of the simulations reported here is to take the simplest imaginable three-dimensional granular system; N monodisperse spheres in a cubic box length L, initially without the complication of gravity, and to examine the obedience of the model to the statistical thermodynamic principle of equipartition of energy and the Maxwell–Boltzmann velocity distribution law.

The equipartition of energy principle requires that a system in thermal equilibrium should distribute the total kinetic energy of all the atoms and/or molecules in that system, on average, equally between all the degrees of freedom of the system. In a granular sphere system in three dimensions with fixed total momenta, there are $3N - 3$ translational and, additionally for rough spheres, $3N$ rotational energies which can fluctuate; i.e. $\sim 6N$ degrees of freedom. The equipartition principle requires that $\frac{1}{6}$ of the total kinetic energy should, on average, reside in each mode of motion.

The concept of 'granular temperature' which, unfortunately, has been widely used previously to describe the kinetic energy function of state, implies a corresponding states scaling relationship to thermal fluids. A subsequent question addressed here, therefore, is: can the properties of this model granular material be predicted from the known properties of the classical hard-sphere fluid? If so, what are the corresponding state scaling laws that will enable the calculation of granular 'thermodynamic properties', such as the steady-state energy? Also of interest is the development of constitutive transport relations for the computational fluid dynamics (CFD) simulation of real granular processes. How are the granular transport coefficients of kinetic energy, mass and momentum in the granular and thermal systems of spheres, respectively, related?

2. Model and simulation methods

The simulation model comprises a fixed number (N) of inelastic spheres confined within the rigid inelastic walls of a uniaxially shaking box (figure 1(a)) which shows how the box is physically shaken. The oscillating amplitude of the box is a 'saw-tooth' wavefunction (figure 1(b)) as described in greater detail previously (Knight 1993). The wall velocity

(v_w) remains fixed as a constant condition of a particular steady state, and relates to the amplitude (λ), and the frequency (ω), according to

$$v_w = 4\lambda\omega.$$

Frequency and amplitude cannot, therefore, both be varied independently when the wall velocity is fixed. When the only time scale in the model is $1/\omega$, and all distances are reduced by the particle diameter σ, the state (or steady state) of the system is uniquely determined by the specification of either a reduced amplitude or a reduced velocity, i.e. both λ and v_w cannot vary independently.

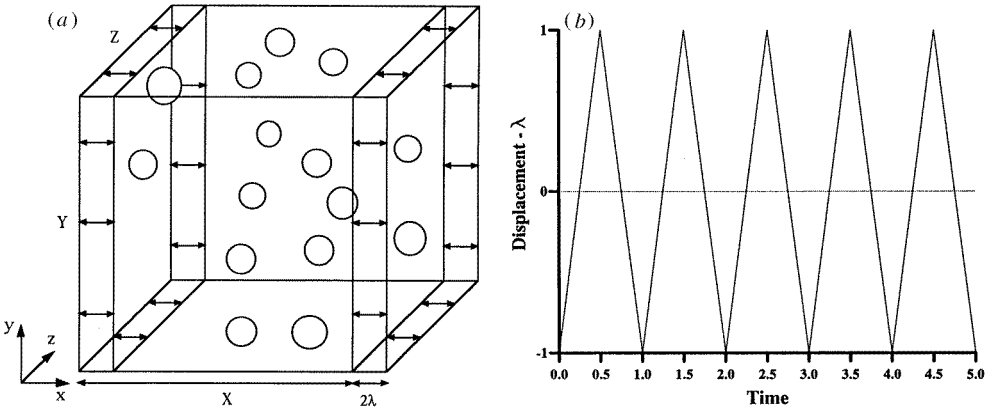

Figure 1. The saw-tooth shaker. The granular spheres are placed in a vibrating cube (*a*), and the cube is shaken at constant velocity and at a steady state with the displacement (λ) given by the saw-tooth form as shown in (*b*).

Simulations have been performed by making changes to a conventional hard-sphere fluid molecular dynamics program (Alder and Wainwright 1960), by considering a fixed-width system within the two bandwidths along the axis of motion, say the x-direction. Only one bandwidth needs to be considered to specify the model. A simple reversal of the following explanation, as defined for the far X-wall, completely specifies the model granular system.

There are three distinct types of particle–wall collision which can occur inside the defined band. Firstly there is the on-coming collision in which an increase in particulate energy is observed; secondly, there is an off-going collision in which a particle velocity is damped, and finally a double collision, where the net energy transfer is either zero or positive. A double collision may occur when an off-going collision causes a particle's trajectory to remain within the band for a sufficient interval to allow a second on-coming collision.

The exact procedure for calculating the wall collision time t_w of a particle with a moving wall is given in detail elsewhere (Knight 1993). Briefly, the process involves splitting the time interval into three separate units as follows:

$$t_w = t_A + t_B + t_C.$$

t_A denotes the time for a particle to reach the lower limit σ_L (in the case of the upper band) of the defined band from

$$t_A = \frac{((\sigma_L - \sigma/2) - r_x)}{v_x} \tag{1}$$

which applies to the first particle–wall collision time as if this limit were a stationary wall, as defined below; in equation (1), r_x is the x-coordinate of the particle, v_x is the component of velocity in the x-direction and σ is the diameter of the particle. In the case where a particle is already located within this band due to a combination of a wall and particle collision or as in the case of a double collision, t_A is then set to zero. If a collision occurs before the wall reaches its turning point σ_H then t_B is calculated from

$$t_B = \frac{(r_\mathrm{w} - (\sigma_\mathrm{L} - \sigma/2))}{v_\mathrm{w} - v_x} \tag{2}$$

where r_w denotes the wall position at time t_A. Equation (2) represents the second time interval.

If, however, the wall reaches its turning point before the collision occurs, t_B then takes the value of the time remaining to get the wall to its turning point and the particle is moved accordingly. The final time t_C (normally set at zero) then comes into play which is found in the same manner as in equation (1) to give the third and final component of the collision.

The final modification is to compute the change in the x-component of the particulate velocities when undergoing wall collisions. Remembering that the wall velocity is a positive constant as defined above, all three possible types of collision are shown in equation (3) below and, although the kinetic energy within the system is free to fluctuate, the equations must abide by the conservation of momentum laws and the respective velocities after collision are as follows:

Type of collision	Change in velocity	
On-coming collision	$v_x = -\varepsilon_\mathrm{w} v_x - (1 + \varepsilon_\mathrm{w}) v_\mathrm{w}$	(3*a*)
Off-going collision	$v_x = -\varepsilon_\mathrm{w} v_x + (1 + \varepsilon_\mathrm{w}) v_\mathrm{w}$	(3*b*)
Double collision	$v_x = \varepsilon_\mathrm{w} v_x - (1 + \varepsilon_\mathrm{w}) v_\mathrm{w}.$	(3*c*)

ε_w is a constant coefficient of restitution in particle–wall collisions. In the simulations here, ε_w is 1, i.e. the particle–wall collisions are elastic.

3. Spheres with elastic collisions

When both the particle–wall and the particle–particle coefficients of restitution are unity, all collisions are elastic and the saw-tooth shaker puts energy into the system by on-going wall collisions faster than it is taken out by some off-going wall collisions. The net result is that the kinetic energy, i.e. the 'granular temperature', of the particles increases *ad infinitum* and a constant kinetic energy steady state is unachievable.

The rate of increase of E^* as a function of time can be predicted analytically from kinetic theory of gases or, more precisely, from Z, the pressure equation of state of the hard-sphere fluid at the same number density as the spheres in the shaking box. The number density of the system (ρ) is defined as $N\sigma^3/V$ and as the packing fraction y is defined as $\pi\rho/6$, a density of 1 corresponds to a packing fraction of $\pi/6$. The particle–wall and particle–particle collision frequencies are given exactly according to kinetic theory by Turner and Woodcock (1992) and in appendix B, respectively, as

$$\Phi_\mathrm{P} = 3(Z - 1)/\sqrt{\pi}$$
$$\Phi_\mathrm{W} = \rho Z/(2\sqrt{\pi}).$$

These collision frequencies are evaluated by calculating Z from a hard-sphere fluid equation of state, e.g. the Carnahan–Starling equation (Carnahan and Starling 1969)

$$Z_{\mathrm{cs}} = \frac{pV}{NkT} = \frac{1 + y + y^2 - y^3}{(1-y)^3}.$$

The evaluation of the rate of energy input for a saw-tooth shaker is derived in appendix A.1. This theoretical calculation assumes that the granular system obeys the equipartition of energy principle and also the Maxwell–Boltzmann distribution law. The obedience to the equipartition principle is first tested for spheres with perfectly elastic collisions.

3.1. Equilibration times

For perfectly elastic spheres, with every increasing energy with time, once the system has come to equilibrium with the saw-tooth shaker, there is no 'new physics' as time progresses. A quasi-steady state is reached when there is no further tendency for the system to apportion its (ever-increasing) energy differently. This may or may not be in accordance with the equipartition principle and is tested below.

It is apparent that there are two dominant factors which influence the time for the system to reach equipartition, namely the density and speed of oscillation, and any increase in either of these gives rise to faster equilibration times.

The behaviour observed as a function of density is simply explained by the increased particle–particle collision frequency Φ_{P}. At higher densities the mean free path, i.e. the average distance between successive particle collisions, is shortened. This allows the ratio of $\Phi_{\mathrm{P}}/\Phi_{\mathrm{W}}$ to increase, which causes more dissipation of energy and therefore faster equilibrium times. At a constant density, however, one might expect that faster oscillations should induce instability and longer equilibrium times as there is more energy being channelled into the x-direction. Precisely the opposite effect is found: as the wall speed increases, so do the particle speeds, which has the effect of lowering the collision times between all particle pairings and therefore increasing the collision rate Φ_{P} which in turn enables equilibrium to occur much faster than for slower oscillations. The graph shown in figure 2 compares equilibrium times found throughout the density range at various shaking amplitudes from 1% to 90% of the box length. The results show that the only region in which a quasi-steady state cannot be accessed on a reasonable time-scale is at very low shaker speeds in very low densities. At all amplitudes up to the order of one box length, equipartition prevails.

3.2. Equipartition at very large amplitudes

An interesting question is: at what point of increasing the amplitude at very high amplitudes, up to many times the box length, will equipartition not be obeyed and how will the energy redistribute itself? One might expect, for example, that at a sufficient amplitude all the kinetic energy might reside in the direction of shaking. This is not found to be the case.

Figure 3 compares two simulations at the large amplitudes of 1 and 100 box lengths to show the variation in the percentage of energy contained in the x degree of freedom, i.e. the direction of shaking. The larger the amplitude of oscillation, the more pronounced the behaviour becomes.

This extraordinary effect may be explained by making reference to a simple impact oscillator with elastic walls as described by Pippard (1985). This model shows that a particle can move in phase with the box and also drastically change its speed by a succession of

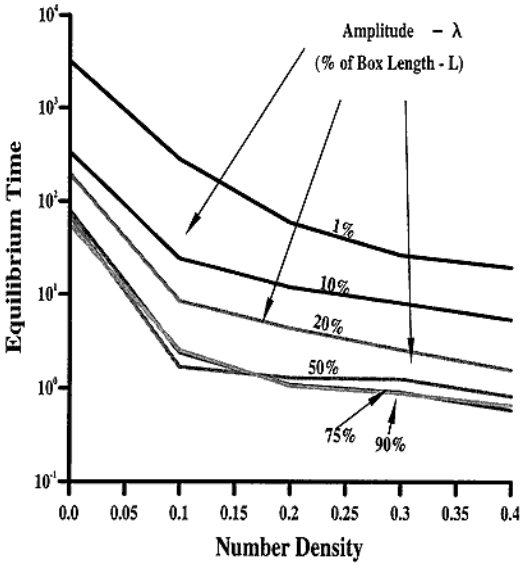

Figure 2. Equilibration times for different amplitudes of shaking (as a percentage of box length) as a function of density. The dimensionless unit of time is one cycle of the saw-tooth shaker.

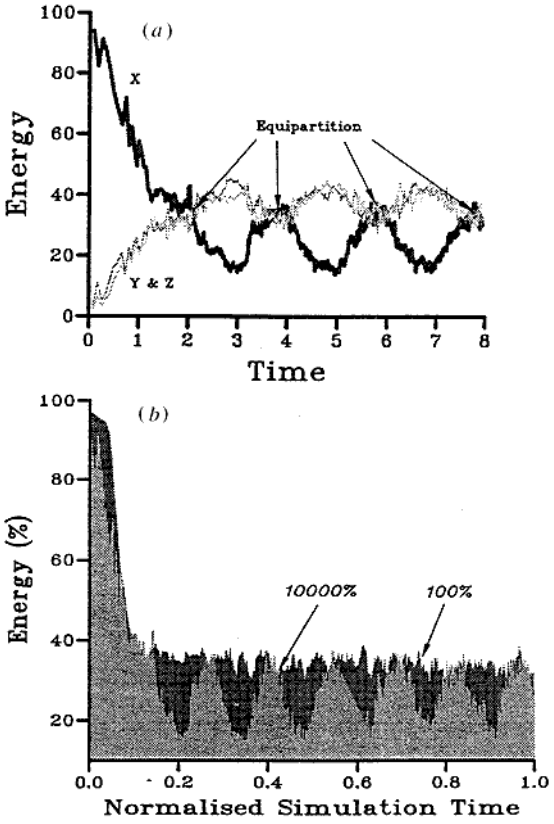

Figure 3. Distribution of kinetic energies between the three Cartesian degrees of freedom in the steady-state vibrating rigid box model at zero gravity; (*a*) for very large amplitudes, oscillatory deviations from instantaneous obedience to equipartition are seen but the time-averaged steady-state kinetic energies still obey the equipartition principle, and (*b*) a comparison between two amplitudes showing that when below ten box side lengths, equipartition is continuously obeyed.

on-coming or off-going collisions. By examination of the Pippard impact oscillator (Knight 1993) it can be seen that when an amplitude above one box length is used, the behaviour, if stable, must repeat over each wavelength. When considering a three-dimensional system,

the same behaviour can occur and the x degree of freedom acts in phase with the box and may incur a large swing in its value. The in-phase oscillations of the normal degrees of freedom, in figure 3, are merely a consequence of plotting the y, z energies as a percentage of the total.

4. Equipartition with rotational spin

4.1. Rotational equations of motion

In a collision between two non-rotating spheres (figure 4) a normal impulse is generated which governs the post-collisional velocities of the colliding pair. In a collision between two rotating spheres, two impulses are present: the normal, created as before by the relative translational velocities, and a tangential component which is produced by the relative angular velocities. The post-collisional velocities involve combining both the normal and tangential components in various ratios to allow the simulation of spheres ranging continuously from perfectly smooth to fully rough.

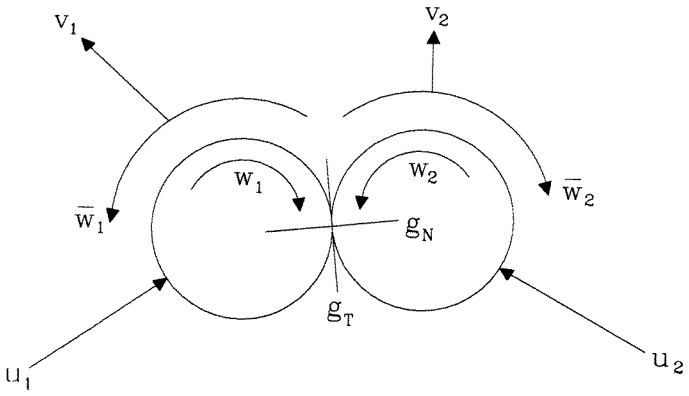

Figure 4. Simple model for inelasticity in rotational collisions.

The equipartition theorem states that each degree of freedom must have an energy of $kT/2$; in this case the total rotational energy is

$$\tfrac{1}{2}m(v_x^2 + v_y^2 + v_z^2) + \tfrac{1}{2}I(w_x^2 + w_y^2 + w_z^2) = 3kT$$

where I is the moment of inertia, which for a sphere is

$$I = \tfrac{2}{5}m\sigma^2$$

and w_x, w_y and w_z are the independent angular velocities which define the exact magnitude and direction of spin of a sphere.

Manipulation of the redefined equations for the conservation of momentum and energy, or by following the procedure outlined by Goldsmith (1960) (see also Chapman and Cowling 1970) yields v and $\bar{w}$, the new post-collisional velocities in terms of the initial impact velocities as given by equations (4)–(8) below for a collinear impact (figure 4):

$$v_1 = u_1 - 4m_2\Delta_A \tag{4}$$

$$v_2 = u_2 + 4m_1\Delta_A \tag{5}$$

$$\bar{w}_1 = w_1 - 10m_2\Delta_A/\sigma_1 \tag{6}$$

$$\bar{w}_2 = w_2 - 10m_1\Delta_A/\sigma_2 \tag{7}$$

where

$$\Delta_A = (u_1 - u_2 + w_1\sigma_1 + w_2\sigma_2)/7(m_1 + m_2). \tag{8}$$

These equations, which are calculated for all six defined velocities for three dimensions, represent the case initially proposed by Bryan (1894) and Pidduck (1922) for a perfectly rough sphere where the tangential and normal impulses, g_T and g_N, are completely reversed after impact. To simulate partially rough spheres, a roughness coefficient (β) is introduced (Lun and Savage 1987), to model partial surface friction. β is used in a similar manner to the coefficient of restitution ε, but models the tangential impact more effectively by its ability to vary between -1 and 1, which relate to simulations involving perfectly smooth and perfectly rough spheres respectively.

4.2. Equations for frictional-wall collisions

These equations are obtained (see e.g. Goldsmith 1960) by combining the conservation of angular momentum (equation (9)) with the velocity ratio before and after impact (equation (10)). When a collision with, say, a wall in the y-direction occurs, while v_y is simply reversed as before, and w_y is directionally independent, all the remaining degrees of freedom now contribute to the collision. For both X- and Z-directions, the conservation of angular momentum requires that

$$I(\bar{w} - w) - m\sigma(v - u) = 0 \tag{9}$$

and the definition of the coefficient of restitution determines the velocity ratio:

$$v + \sigma\bar{w} = -\varepsilon_w(u + \sigma w) \tag{10}$$

where $\varepsilon_w = 1$ for perfectly elastic walls. By manipulating these equations it can be shown that

$$v = u - \frac{(u + \sigma w)(\varepsilon_w + 1)I}{I + m\sigma^2}$$

which on resubstitution gives

$$\bar{w} = w - \frac{m\sigma(u + \sigma w)(\varepsilon_w + 1)}{I + m\sigma^2}$$

where the respective components in the y-direction are

$$v = -u \qquad \text{and} \qquad \bar{w} = -\beta w.$$

If the collision is with a moving wall, the impact is always modelled in the same way but, in this case, the wall velocity must be included in the above calculations. Both the X- and Z-components of spin are affected for a moving Y-wall.

4.3. Equipartition with spin

Equipartition may only be obtained when $\beta = 1$; this models the idealized but unrealistic granular system of perfectly rough and perfectly elastic spheres. For all other values of β, energy is lost during each impact, except for the limiting case when $\beta = -1$, at which point interchange of energy between rotational and translational modes is not allowed and equilibration cannot occur.

As the main purpose of this article is to examine the equipartition theorem during the influence of system vibrations, only the case when β is unity is considered. In this limit the equipartition principle requires that the total energy of the system be shared equally

among all six degrees of freedom. Over a wide range of amplitudes, it has been observed that the rotational modes follow very closely their respective translational modes during equilibration, and that equipartition of the whole system does indeed eventually prevail.

To demonstrate this behaviour figure 5 shows plots of all six components of a system of 500 particles, at the reduced density $\rho = 0.5$, being shaken in the x-direction with the amplitude $\lambda = \sigma/10$. In this simulation all the energy of the system is initially placed into both z-components of energy. Complete equipartition is observed after 60 cycles of the shaker. Although the behaviour of the rotational degrees of freedom, compared to the translational degrees, is similar in the latter stages of the simulation, initially, when the system is trying to reach a balance, the differences in the rotational energy components are less than in the translational components. The driving force towards equipartition appears to be even greater amongst the rotational modes than the translational modes.

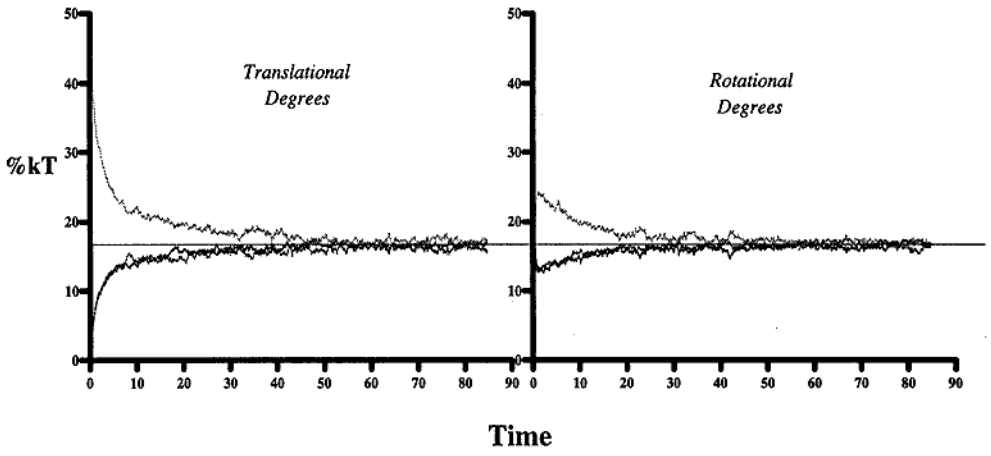

Figure 5. A demonstration of the equipartition of energy in six degrees of freedom, at steady state with uniaxial shaking ($\lambda = \sigma/10$), after initially setting all the energy in the one (Z) translational degree of freedom.

5. Spheres with inelastic collisions

5.1. Dependence of the granular energy

When the energy input from the saw-tooth shaker walls is balanced by the dissipation of energy through inelastic collisions, a steady state of constant kinetic energy, which actually fluctuates slightly about a mean value, is obtained. At low amplitudes equipartition prevails, and the mean kinetic energy per sphere (E) stays constant. A reduced kinetic energy per sphere, defined as

$$E^*(\rho, v_w, \varepsilon) = E/(m\sigma^2\omega^2)$$

at a given density (ρ), is a function only of the wall velocity (v_w), and the constant of inelasticity (ε). E actually scales with the wall velocity (mv_w^2) and the reduced granular energy (E^*) is independent of the wall velocity.

When either the particle–wall or the particle–particle collisions are inelastic, with a prescribed coefficient of restitution, the shaker equilibrates to a steady state with a total

kinetic energy per particle E that depends only on the density (ρ), wall velocity (v_w) and the inelasticity constant (ε).

The rate at which energy is removed from the system by inelastic particle–particle collisions can be calculated from the collision rate (appendix A.2). This dissipation rate may then be used in an energy balance equation for inelastic spheres to solve for the steady-state granular temperature E^* as a function of the granular steady-state variables.

The thermal kinetic energy of the system in equations (A3) and (A5) is equivalent to kT, where k is Boltzmann's constant. In the saw-tooth shaker energy balance, kT becomes the *a priori* unknown granular kinetic energy E. This quantity is commonly, but inappropriately, often referred to as a 'granular temperature'. When expressed in saw-tooth units as above, E^* can be computed analytically for saw-tooth systems at low amplitude that obey the equipartition principle by solving the energy balance equation. At steady state, $\Delta E_{in} = \Delta E_{out}$ and the respective ΔE's are given in appendix A by equations (A3) and (A5). The resultant energy-balance master equation is

$$\frac{\rho Z}{2\sqrt{\pi}}\left\{2v_w[1-e^{-mv_w^2/(2E)}]\left[\frac{2mE}{\pi}\right]^{1/2}+4mv_w^2\left[1-\tfrac{1}{2}\,\mathrm{erf}\left(v_w\sqrt{\frac{m}{2E}}\right)\right]\right\} = \frac{3(Z-1)(1-\varepsilon^2)E}{\sqrt{\pi}}. \tag{11}$$

This equation can be solved (using 'solver' on an EXCEL spreadsheet for example) to determine the granular kinetic energy E for any given density, velocity and inelasticity constant for the saw-tooth shaker. This energy balance equation further implies that the energy in reduced units of the saw-tooth system, i.e. E^*, is not dependent on frequency or amplitude and should, according to this theory, obey the equipartition laws in *the limit of small amplitude*. This theoretical prediction follows from the absence of any explicit amplitude dependence of the granular energies in the energy balance equation (11).

It should be noted that E^*

(i) does not itself depend upon that amplitude, and
(ii) obeys the equipartition principle, i.e. the kinetic energy is distributed evenly amongst the degrees of freedom despite the unidirectional nature of the shaking.

The extent to which these assertions are upheld, for small finite systems at finite amplitudes, is examined below. The simulations reported in the previous section have already demonstrated a total obedience of equipartition of a system of frictional spheres with six degrees of freedom, at the amplitude of $\lambda = \sigma/10$.

For a given value of the inelasticity coefficient (ε), E^* is an irreducible function only of reduced number density for granular inelastic spheres shaken at low amplitude. The energy balance equation, however, suggests that in the limit $\varepsilon \to 1$ the dependence on inelasticity may also scale out as $(1-\varepsilon)^{-1}$. It has been demonstrated recently by Warr and Huntley (1995b) that for a single particle in a saw-tooth shaker $E^*(1-\varepsilon)^{-1}$ is constant. This scaling law is not exact for a many-body system but its applicability can be tested over a range of ε from the present simulation data.

The calculated values of E^* over the whole range of ε are shown in figure 6. As $\varepsilon \to 0$, this is the maximum rate of energy extraction by inelastic collisions and E^* converges on to a limiting function of density. $E^*/(1-\varepsilon)$ does appear to hold quite well for low values of ε but deviates from a constant value as ε approaches unity, i.e. as E^* approaches infinity. E^* and the relaxation times for equilibration diverge to infinity, both as density goes to zero and/or as ε approaches unity.

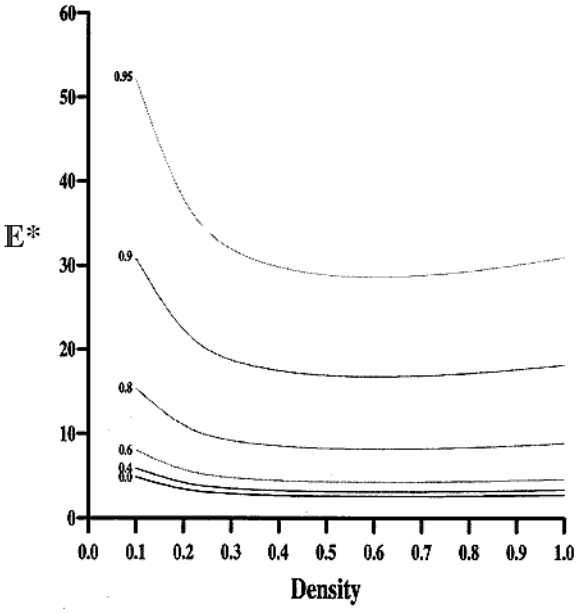

Figure 6. E^* (the reduced granular energy $= E/(m\sigma^2\omega^2)$) as a function of density for a range of ε values as given by the hard-sphere fluid corresponding states scaling theory; when $\varepsilon \to 1$, $E^* \to$ infinity, and as $\varepsilon \to 0$, $E^*(\rho, \varepsilon) \to$ a constant minimum value.

At high density, which is more important for dense granular media, E^* appears to approach a limiting constant value around 4. Since the saw-tooth velocity is also 4, in saw-tooth units, when $\lambda = 1$ and $\omega = 1$, this suggests that, in the high density limit, the root mean squared velocity of all the particles becomes the same as that of the saw-tooth shaker, i.e. v_w. This may become an analytic result in the limit of maximum close packing, amorphous or crystalline.

5.2. Equipartition at low amplitude

The results of the computer simulations, additional to the analytical energy balance, confirm that the granular energy of the fluidized spheres depends only on the shaker velocity, and not the amplitude or frequency. The condition for the energy balance to hold, however, is that the amplitude is small compared to the mean velocity of the particles.

A series of computer simulations have been carried out for various saw-tooth amplitudes ($\lambda = 1$, 0.5, 0.25 and 0.1), for $N = 100$ and 500, over the whole density range, and for a value of the inelasticity constant $e_p = 0.9$ for particle–particle collisions. Details of all these simulations, together with the granular kinetic energies, resolved into the translational components, are collected in table 1.

The results of this comparison between theory and simulation are compared in figure 7. The energy balance equation has been tested by comparing the calculated energy from the computer simulations with the predicted granular energy obtained by solving the kinetic energy balance equation (11). The comparisons in figure 7 show that, over the whole accessible density range of the simulations, the analytical kinetic theory prediction is accurate but it is not exact. The computer results show a more complex behaviour of E^*, particularly at intermediate densities; the theoretical prediction is a single minimum at

Table 1. List of simulation steady states investigated showing the total granular energy E^* and its three degrees of freedom which define the equipartition ratio (Γ) for two system sizes ($N = 100$ and $N = 500$); these numerical results verify that an increase in either the number density or amplitude reduces Γ, implying increased deviations from the equipartition principle.

Run	N	λ^*	ρ^*	Colls	E^*	E^*_{xx}	E^*_{yy}	E^*_{zz}	Γ
1	100	1	0.01	600 000	569.498 ± 14.87	202.77	182.85	183.79	0.97
2	100	1	0.1	50 000	115.745 ± 6.13	43.27	36.39	36.07	0.94
3	100	1	0.2	50 000	64.4427 ± 3.53	25.69	19.44	19.30	0.90
4	100	1	0.3	50 000	43.7566 ± 0.87	18.79	12.54	12.42	0.86
5	100	1	0.4	50 000	24.6507 ± 1.53	14.33	8.73	8.71	0.82
6	100	1	0.5	100 000	24.6507 ± 0.71	11.71	6.48	6.45	0.79
7	100	1	0.6	100 000	19.9087 ± 0.59	9.38	4.95	4.91	0.77
8	100	1	0.7	250 000	17.0467 ± 0.77	8.52	4.28	4.24	0.75
9	100	1	0.8	150 000	15.9667 ± 0.57	8.27	3.84	3.85	0.72
10	100	1	0.9	800 000	14.7067 ± 0.18	7.81	3.58	3.31	0.70
11	100	1	0.93	350 000	11.9000 ± 0.47	6.77	2.57	2.55	0.65
12	500	1	0.01	900 000	181.030 ± 67.0	64.88	58.22	57.93	0.96
13	500	1	0.1	100 000	37.1886 ± 1.13	13.36	11.94	11.89	0.96
14	500	1	0.2	150 000	20.4441 ± 0.71	7.43	6.54	6.47	0.95
15	500	1	0.3	200 000	14.7445 ± 0.55	5.45	4.64	4.65	0.95
16	500	1	0.4	375 000	16.5450 ± 0.70	6.59	4.94	5.01	0.90
17	500	1	0.5	700 000	19.9170 ± 0.44	8.86	5.51	5.54	0.83
18	500	1	0.6	850 000	19.9941 ± 0.80	9.46	5.26	5.27	0.79
19	500	1	0.8	800 000	16.4297 ± 0.52	8.79	3.83	3.80	0.70
20	500	1	0.9	600 000	15.4113 ± 1.32	8.46	3.46	3.49	0.68
21	500	1	0.99	550 000	13.8115 ± 0.52	7.89	2.97	2.95	0.64
22	500	0.5	0.6	100 000	2.94666 ± 0.12	1.11	0.91	0.91	0.93
23	500	0.5	0.9	200 000	5.30110 ± 0.29	2.53	1.39	1.39	0.79
24	500	0.25	0.6	100 000	0.73966 ± 0.03	0.27	0.24	0.23	0.95
25	500	0.25	0.9	100 000	0.95775 ± 0.05	0.38	0.29	0.29	0.90
26	500	0.01	0.4	250 000	0.00139 ± 0.0001	0.00049	0.00045	0.00046	0.98
27	500	0.01	0.9	250 000	0.00126 ± 0.0001	0.00045	0.00041	0.00041	0.97

a density around 0.5.

It seems likely that the main reason for the discrepancy between theory and experiment is due to finite-size effects in the granular simulations. Other reasons for small deviations may be the finite amplitude relative to the size of the box and/or the correlation length of the particles. For small systems, at finite amplitudes, there is a greater likelihood of either double or multiple successively correlated collisions with the same particle. These distort the distribution assumed by the simple Maxwellian distribution model based on the collision frequencies of the hard-sphere fluid at equilibrium.

5.3. Non-equipartition at high amplitudes: the equipartition ratio

An equipartition ratio can be defined by

$$\Gamma = \frac{3(E_{yy} + E_{zz})}{2E}.$$

For all the simulations carried out, the equipartition ratios are given in table 1. Taking a particular density of, say, 0.9; when λ varies between 0 and σ, then just as Γ (the difference in translational modes) increases, a similar difference operator is needed to describe the variation seen in the rotational modes. Whereas at $\lambda = \sigma$ both the translational and rotational

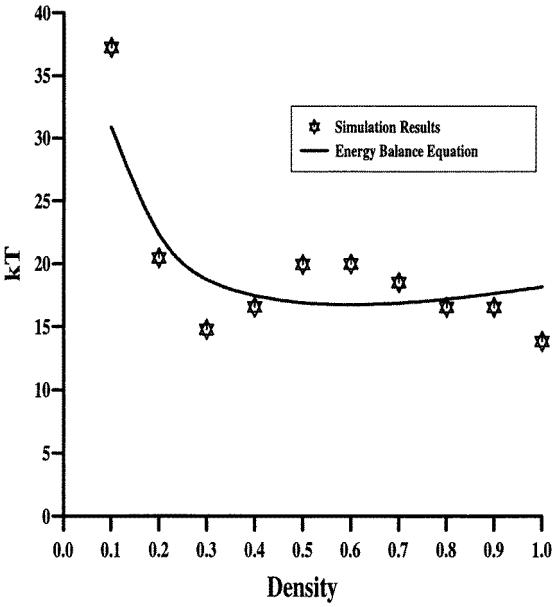

Figure 7. A comparison between the corresponding states theory for E^* (full curve) and the computer simulation results at selected densities (asterisks). At this amplitude for the simulations ($\lambda = \sigma$) the comparisons show small but significant deviations from equipartition at intermediate and high densities.

modes in the direction of vibration now take up more energy than the accompanying modes, when λ is small, Γ diminishes and the system reverts to one of equipartition. This result for the effect of finite amplitude on the equipartition ratio is shown, for this state point, in figure 8. The equipartition ratio approaches unity as $\lambda \to 0$ and appears to approach $\frac{2}{3}$ as the amplitude increases to σ.

The results in table 1 also demonstrate a significant system size effect. Figure 9 shows the equipartition ratio plotted against the characteristic length of the system, i.e. the length (L) of the side of the box, over the whole density range. For the smaller number of particles at the same box length, equipartition holds better. This implies that it is not primarily the amplitude relative to the box length that determines the extent of non-equipartition, but the ratio of the amplitude to a characteristic path length for the structure of the particles at steady state, that increases with density.

If a characteristic path length is simply defined as $\Lambda = \rho^{-1/3}$, the results plotted in figure 10 confirm that this is indeed the case. At both high and low path lengths the two different system sizes show much the same non-equipartition extent. These results suggest that provided the system size is at least several hundred particles, the criterion for the obedience of the equipartition principle is that the ratio of the amplitude to a mean path length

$$\lambda/\Lambda$$

should be less than unity for the equipartition of kinetic energy.

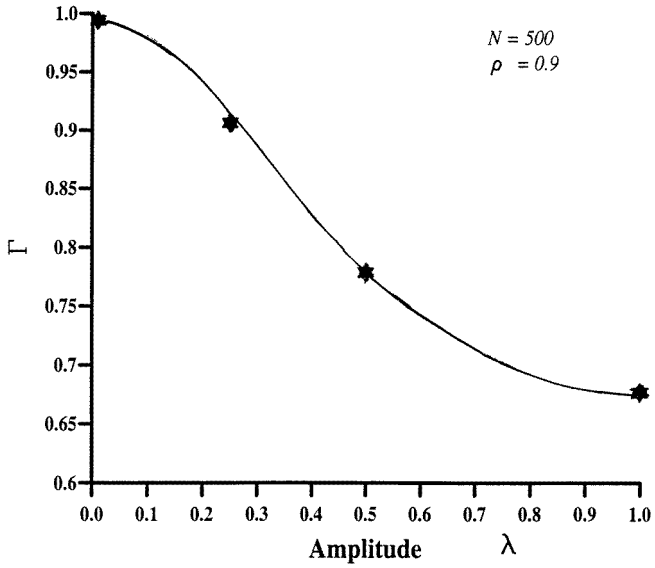

Figure 8. The equipartition ratio (Γ) as a function of amplitude for a system of 500 spheres with a saw-tooth shaker at constant velocity for inelastic spheres ($\varepsilon = 0.9$).

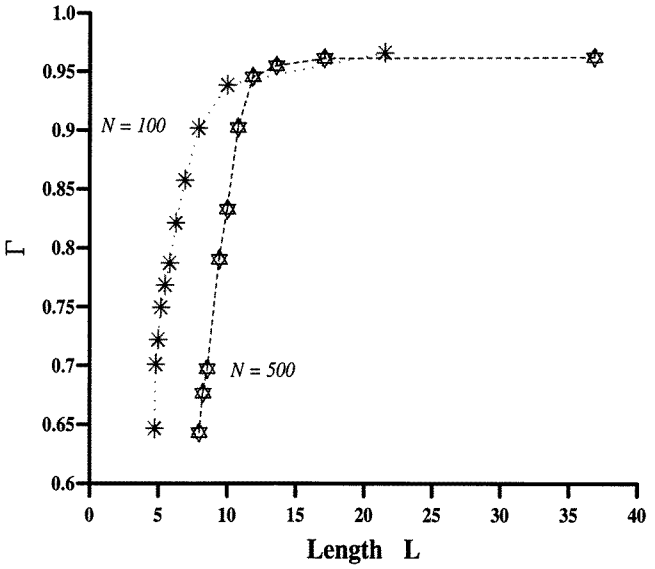

Figure 9. The equipartition ratio (Γ) as a function of box length (L) for systems of 100 and 500 inelastic spheres ($\varepsilon = 0.9$).

5.4. Maxwellian velocity distributions

In addition to testing the equipartition of energy principle, the steady states of the system have been investigated for the actual distribution of velocities in the directions transverse and longitudinal to the shaker wall velocity. Molecular systems in thermal equilibrium, besides adhering to the equipartition principle, distribute the molecular velocities according

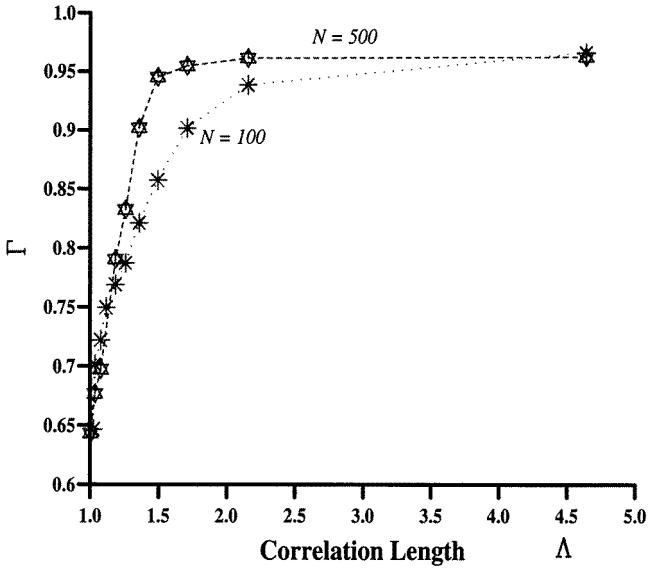

Figure 10. The equipartition ratio (Γ) as a function of correlation length (Λ) for systems of 100 and 500 inelastic spheres ($\varepsilon = 0.9$).

to the Maxwell–Boltzmann distribution law. According to this exact result of kinetic theory, the probability of a molecule having a particular velocity in any component is given by

$$P(v_x) = \left(\frac{m}{2\pi kT}\right)^{\frac{1}{2}} \exp\left(-\frac{mv_x^2}{2kT}\right). \tag{12}$$

This distribution is assumed in the kinetic equations on both sides of the energy balance equation (11). In the energy input from particle–wall collisions with the saw-tooth shaker, a Maxwellian distribution is explicitly assumed for the relative particle–wall velocity. Likewise, in the collisional energy dissipation side of the balance equation, the particle–particle collision frequency is calculated from an equation of state which assumes quasi-thermodynamic equilibrium and hence implicitly assumes a Maxwellian distribution of particle velocities.

The results of comparisons between the Maxwell–Boltzmann distribution law and the actual saw-tooth shaker distributions (in which 'kT' becomes E^*) are illustrated in figure 11. In all simulated states with small amplitude and/or sufficiently low density where equipartition is upheld, a Maxwellian distribution of velocities is obtained. This is illustrated in figure 11(a). Very slight deviations from a Maxwellian distribution are seen at somewhat higher densities when the amplitude is 1σ (figure 11(b)) but when the deviations from equipartition are large, at the higher packing density, the distribution of velocities deviates markedly from the Maxwellian law.

Figure 11(c) shows that at large shaking amplitudes at high densities, the parallel distribution of velocities in the parallel has a flat top, whereas the distribution in the transverse directions is narrower, but very close to the Maxwellian model.

The reasons for the unusual flat-top shape of the longitudinal distribution can be gleaned from the total kinetic-energy–time curves for these three runs, also shown on the right-hand side of figure 11. At sufficiently high amplitude or density, the total kinetic energy begins to fluctuate with the periodicity of the shaker itself, and the x-component of the time average

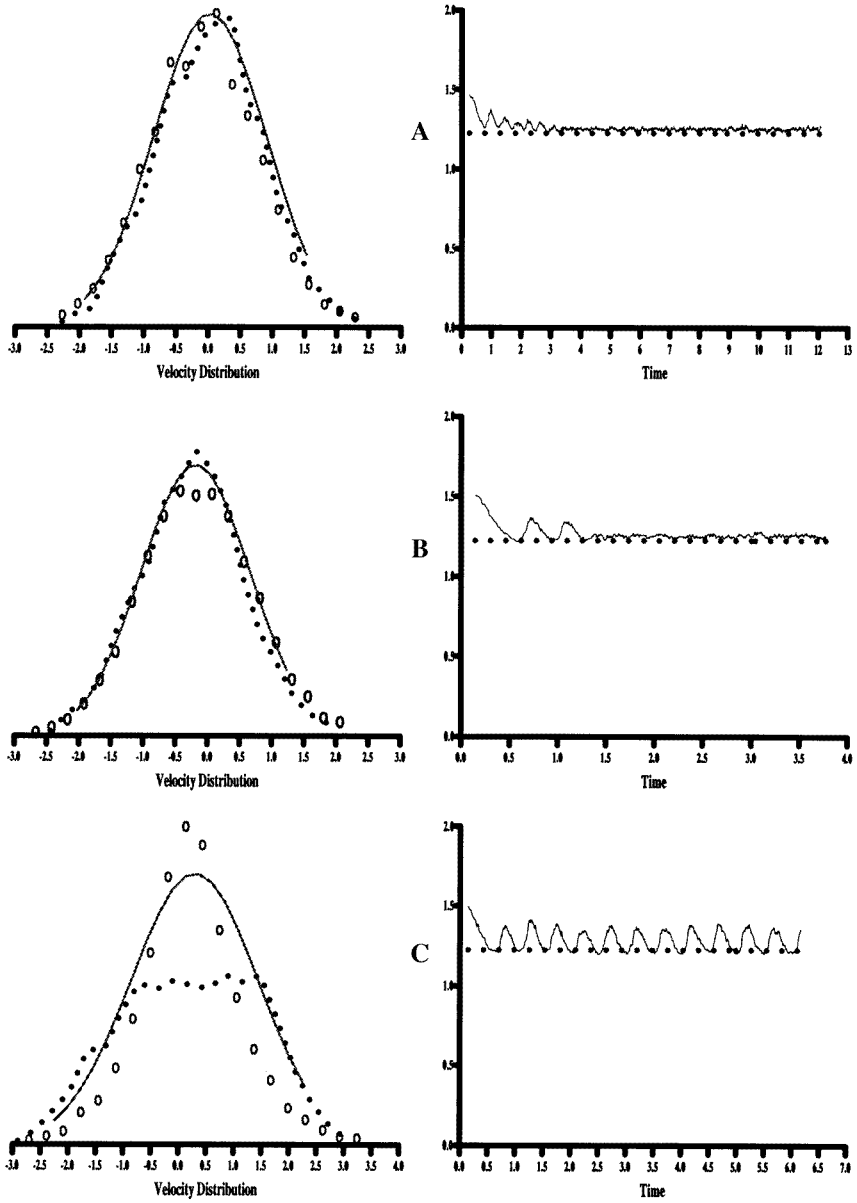

Figure 11. Distributions of absolute velocities particles in the saw-tooth shaker for three different steady states by comparison with a Maxwell–Boltzmann distribution (full curve). (A) Run 26: low amplitude ($\lambda = 0.01$), $\rho = 0.4$; equipartition ratio $= 0.98$. (B) Run 16: large amplitude ($\lambda = 1.0$), $\rho = 0.4$; equipartition ratio $= 0.90$. (C) Run 20: large amplitude ($\lambda = 1.0$), $\rho = 0.9$; equipartition ratio $= 0.68$. The corresponding plots against time on the right are the root mean square speeds.

can be resolved into a convolution of 'mini-Maxwellian distributions' each centred on the absolute velocity of the shaker. This implies that there is a correlation between the wall velocities and the particle velocities.

If a peculiar velocity of the spheres is defined relative to the wall velocities (i.e. $v_r = v - v_w$) one might expect to recover the random Maxwellian velocity distributions even when equipartition does not prevail between transverse and longitudinal directions. Figure 12 shows that this is, at least approximately, the case. It is interesting to note the large discrepancy between the distributions of absolute velocities and relative velocities, especially in the longitudinal direction, when anisotropies in the kinetic energy distribution occur.

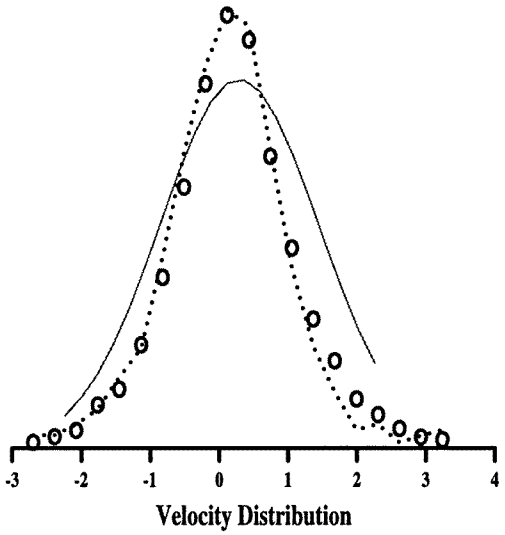

Figure 12. The distribution of relative velocities, with respect to the wall velocity for Run 20, i.e. at large amplitude, $\lambda = 1.0$; $\rho = 0.9$; and equipartition ratio = 0.68, by comparison with a Maxwell–Boltzmann distribution (full curve). This near-Maxwellian contrasts with the flat-top distribution obtained for the absolute velocities as seen in figure 11(*c*).

5.5. Corresponding states scaling laws

From the foregoing treatment and simulation results, it is clear that this fluidized system of spheres has a unique corresponding states relationship with the thermal hard-sphere fluid. In the limit of low amplitude to box length ratio, and for sufficiently large particle number N, i.e. at least several hundred, every state of the saw-tooth fluid has a corresponding state of the hard-sphere fluid.

In both systems the dimensions of mass (m) and length (σ) are the same, and the properties of the granular system at the same density as the hard-sphere fluid will then scale according to the ratio of the respective characteristic times. Once E^* is obtained for a saw-tooth shaker from equation (11), this can be used to calculate any other property of the granular system from the value of that property for the thermal hard-sphere fluid. Of particular interest may be the granular pressure, granular diffusivity, or granular thermodynamic properties such as the entropy. If the classical thermal hard sphere units are mass m, length σ, and $m\sigma^2/(kT)^{1/2}$ for time, denoted by a superscript dagger, and $E^\dagger$ is a constant ($= \frac{3}{2}$) independent of density. For the present granular spheres the scaling laws for the above-mentioned granular properties are:

$$\text{energy} \qquad E^*(\rho, \varepsilon) = E/(m\sigma^2\omega^2) \tag{13}$$

where E is obtained from the energy balance equation (11). Then, granular thermodynamic properties can be calculated from the scaling equations

$$\text{pressure} \qquad p^*(\rho,\varepsilon) = p^\dagger(\rho)E^*(\rho,\varepsilon)/E^\dagger \tag{14}$$

$$\text{entropy} \qquad S^*(\rho,\varepsilon) = S^\dagger(\rho)E^*(\rho,\varepsilon)/E^\dagger \tag{15}$$

and likewise, the transport coefficient relations may also be obtained

$$\text{'thermal' conductivity} \qquad \kappa^*(\rho,\varepsilon) = \kappa^\dagger(\rho)(E^*(\rho,\varepsilon)/E^\dagger)^{3/2} \tag{16}$$

$$\text{diffusivity} \qquad D^*(\rho,\varepsilon) = D^\dagger(\rho)(E^*(\rho,\varepsilon)/E^\dagger)^{1/2} \tag{17}$$

$$\text{viscosity} \qquad \eta^*(\rho,\varepsilon) = \eta^\dagger(\rho)(E^*(\rho,\varepsilon)/E^\dagger)^{1/2}. \tag{18}$$

Equations (13) to (18) are the basic scaling equations for predicting the thermodynamic and transport properties of the saw-tooth granular fluid of inelastic spheres, given the shaker parameters, from the known equation of state, i.e. collision frequencies, of the thermal hard-sphere fluid.

Finally, although the expression 'granular temperature' is really a misnomer for the granular kinetic energy E, and may be largely an irrelevance, it seems curiously interesting to calculate the actual granular temperature of a fluidized hard-sphere media. Adopting the ideal gas as the working substance for the absolute temperature scale, in which case Boltzmann's constant retains its usual value, for a system of 1 cm diameter spheres ($\varepsilon = 0.95$), with mass 1 g, shaken at the rate of 1 cps for an amplitude of 1 cm; if the number density $\rho = 1.0$, from figure 6, $E^* = 32$ therefore $E = 30/4 = 8$ ergs and the granular temperature is 'T' $= 8/k = 6 \times 10^{16}$ K. These granular fluids are quasi-'hot' states indeed! This is the ambient temperature on the absolute scale that would be required to maintain the macroscopic granular system at the same state of thermal activation as the saw-tooth shaker in its gravity free environment.

6. Conclusions

An analytical analysis of a saw-tooth shaker has been presented and tested against computer simulations. It has been shown that granular materials when fluidized by shaking under zero gravity, will, at steady state, obey the equipartition principle of statistical mechanics. This obedience occurs at amplitudes of oscillation which are small compared to a characteristic length for particle–particle structural correlation which is roughly the reciprocal cube root of density.

This observation places the concept of 'granular temperature' on a firm statistical mechanical basis for these systems, and thereby permits the steady-state properties of such matter to be expressed as quasi-thermodynamic functions. Comparisons between the shaker simulation results for low amplitudes, and the kinetic-theory-based energy balance model, show that there exists a corresponding states relationship between the granular steady state, and the thermodynamic state the classical hard-sphere fluid at equilibrium.

The coefficient of inelasticity of real granular materials is extremely difficult, if not impossible, to measure experimentally. The present results suggest that the construction of saw-tooth shakers to examine the total kinetic energy as a function of velocity, initially, albeit in microgravity conditions, could be an experimental means of accessing inelasticity constants for real materials in the form of spherical beads.

It is anticipated that this preliminary research could further lead to the quasi-thermodynamic description of a range of steady-state granular transport phenomena, such as size segregation, in terms of thermodynamic mixing laws for binary systems, for example.

Acknowledgments

We wish to acknowledge the Engineering and Physical Science Research Council for the award of a Research Grant (GR/K/06099); we also thank Dr Stephen Warr for his helpful comments on the content of this paper.

Appendix A. Energy balance equations for a saw-tooth shaker

A.1. Energy gain from wall impacts

One saw-tooth waveform is realized in each time unit; there is always one constantly moving on-coming wall and one simultaneous off-going wall. In essence, the integrals below assume that there are two moving walls, one which is always compressing the system, and another which is acting in the opposite direction.

When a particle moving at a speed u collides with a near-sided on-coming wall moving at a constant v_w, the new velocity, v, of the particle is

$$v = -\varepsilon_w u + (1+\varepsilon_w)v_w$$

and likewise for an off-going wall, the new velocity is given by

$$v = -\varepsilon_w u - (1+\varepsilon_w)v_w$$

where it is assumed that a constant coefficient of restitution (i.e. impact velocity independent) is present during each wall contact. This coefficient of restitution which takes into account the surface of the walls and the material constant of the particles at an average impact velocity of $\langle v_0 \rangle$ is denoted by ε_w and is not to be confused with the previously defined coefficient of restitution ε for particle–particle collisions.

The change in energy that these two walls impart on the system is shown in equations (A1) and (A2) by simply considering the change in kinetic energy before and after each type of impact.

$$\Delta E_{IN} = \frac{m}{2}[v_0^2(\varepsilon_w^2 - 1) + 2\varepsilon_w(1+\varepsilon_w)v_0 v_w + (1+\varepsilon_w)^2 v_w^2] \tag{A1}$$

$$\Delta E_{OUT} = \frac{m}{2}[v_0^2(\varepsilon_w^2 - 1) - 2\varepsilon_w(1+\varepsilon_w)v_0 v_w + (1+\varepsilon_w)^2 v_w^2]. \tag{A2}$$

To get the net increase, a Maxwell distribution of velocities is assumed. $f(v_x)$ represents the x-component of a particulate velocity, and is given by

$$f(v_x)\,\mathrm{d}v_x = \left[\frac{m}{2\pi kT}\right]^{1/2} \mathrm{e}^{-mv_x^2/2kT}\,\mathrm{d}v_x$$

and an integration over the whole range of velocities is then performed. It should be noted that when integrating for the off-going wall, a lower limit of v_w is used as no wall collisions may occur unless a particulate velocity is greater than the wall velocity.

$$\begin{aligned}\Delta E = \frac{m}{2}\left(\frac{m}{2\pi kT}\right)^{\frac{1}{2}} \int_0^\infty [&(v^2(\varepsilon_w^2 - 1) + 2v\varepsilon_w(1+\varepsilon_w)v_w \\ &+(1+\varepsilon_w)^2 v_w^2)\mathrm{e}^{-mv_w^2/(2kT)}]\,\mathrm{d}v \\ &+\frac{m}{2}\left(\frac{m}{2\pi kT}\right)^{\frac{1}{2}} \int_{v_w}^\infty [(v^2(\varepsilon_w^2 - 1) - 2v\varepsilon_w(1+\varepsilon_w)v_w \\ &+(1+\varepsilon_w)^2 v_w^2)\mathrm{e}^{-mv_w^2/(2kT)}]\,\mathrm{d}v.\end{aligned}$$

The evaluation of these integrals gives

$$\Delta E = v_w(1+\varepsilon_w)[2\varepsilon_w - (1+\varepsilon_w)e^{-mv_w^2/(2kT)}]\left[\frac{mkT}{2\pi}\right]^{1/2} + mv_w^2(1+3\varepsilon_w^2) + 2(\varepsilon_w^2-1)kT$$
$$-\tfrac{1}{2}\,\mathrm{erf}\left(v_w\sqrt{\frac{m}{2kT}}\right)[mv_w^2(\varepsilon_w+1)^2 + (\varepsilon_w^2-1)kT]$$

which can be simplified by setting ε_w at 1 for the case of elastic walls

$$\Delta E = 2v_w[1-e^{-mv_w^2/(2kT)}]\left[\frac{2mkT}{\pi}\right]^{1/2} + 4mv_w^2\left[1-\tfrac{1}{2}\,\mathrm{erf}\left(v_w\sqrt{\frac{m}{2kT}}\right)\right]. \tag{A3}$$

The final expression for the wall energy input ΔE_{in} is therefore obtained by multiplying equation (A3) by Φ_W, the wall collision rate per particle per moving surface which is defined in appendix B.

A.2. Energy loss by inelastic collisions

The mean energy loss in particle–particle collisions is given by

$$\Delta E = \frac{m(1-\varepsilon^2)\langle v_0^2\rangle}{4} \tag{A4}$$

where $\langle v_0\rangle$ is the average impact velocity of a particle and ε is the constant of inelasticity.

To obtain the net energy loss per particle, this quantity has to be multiplied by the particle–particle collision frequency (Φ_P) and divided by the number of particles in the system (N). Also as the impact velocity is related to the mean speed according to kinetic theory by:

$$\langle v_0^2\rangle = \frac{4\langle v^2\rangle}{3} = \frac{4(3kT/m)}{3} = \frac{4kT}{m}.$$

On substituting into equation (A4)

$$\Delta E = \frac{\Phi_P(1-\varepsilon^2)kT}{N}.$$

As it can be shown (Turner and Woodcock (1990)) that Φ_P per particle is $3(Z-1)/\sqrt{\pi}$ where Z is the reduced pressure equation of state (pV/NkT) for the thermalized system, the resulting energy loss per particle can be expressed as

$$\Delta E = \frac{3(Z-1)(1-\varepsilon^2)kT}{\sqrt{\pi}}. \tag{A5}$$

Appendix B. Calculation of the wall collision frequency

The pressure of the hard-sphere fluid at equilibrium is related to the collision frequency of wall collisions via the equation of state of the system as shown below.

On each impact with a wall, a change in momentum of $2m\langle v_0\rangle$ occurs where $\langle v_0\rangle$ denotes the average impact velocity of a particle.

It therefore follows that the pressure is given by

$$p = 2m\langle v_0\rangle\Phi_W$$

where Φ_W is the total number of collisions per particle with the wall, per unit area in each time unit.

As the equation of state is defined as

$$Z = \frac{pV}{NkT}$$

it then follows that the wall collision fequency x momentum exchange equates to the premiere, and is given by

$$\Phi_{\mathrm{W}} = \frac{NZkT}{2m\langle v_0\rangle V}.$$

As $\langle v_0\rangle = (\pi kT/m)^{1/2}$ and substituting Φ_{W} for the corresponding $\Phi^{\dagger}_{\mathrm{W}}$ to convert into hard-sphere units, as given by

$$\Phi^{\dagger}_{\mathrm{W}} = \Phi_{\mathrm{W}}\sigma^2\left(\frac{m\sigma^2}{kT}\right)^{1/2}$$

it follows that

$$\Phi^{\dagger}_{\mathrm{W}} = \rho Z/2\pi^{1/2}$$

where ρ denotes the number density $N\sigma^3/V$, or by defining $p\sigma^3$ as the reduced pressure $p^{\dagger}$, we have

$$\Phi^{\dagger}_{\mathrm{W}} = p^{\dagger}/2\pi^{1/2}.$$

Appendix C. Nomenclature

β	roughness coefficient
ε	constant coefficient of restitution for particle collisions
ε_{w}	constant coefficient of restitution for wall collisions
Γ	equipartition ratio
Φ_{P}	particle–particle collision frequency per particle
Φ_{W}	partial–wall collision frequency per particle
ρ	number density $(N\sigma^3/V)$
σ	particle diameter
λ	amplitude of saw-tooth wave
ω	frequency of saw-tooth wave
E	kinetic energy per particle
E^*	kinetic energy saw-tooth reduced units
$E^{\dagger}$	kinetic energy thermal hard-sphere reduced units
E_{xx}	x-directional kinetic energy
E_{yy}	y-directional kinetic energy
E_{zz}	z-directional kinetic energy

g_{N}	normal impulse in a particle–particle collision
g_{T}	tangential impulse in a particle–particle collision
N	number of particles in system
p	pressure
I	moment of inertia for a sphere
r_{w}	wall position
r_x	x particle coordinate
t_A	first time component; particle to lower band limit
t_B	second time component; band limit to wall/turning point
t_C	third time component; turning point to wall
t_{w}	collision time for a particle and a moving wall
u	initial velocity prior to impact
V	volume
v_{w}	wall velocity
$v_{x,y,z}$	x, y, z particulate translational velocities
$\langle v \rangle$	mean speed
$\langle v_0 \rangle$	impact velocity
$w_{x,y,z}$	x, y, z particulate angular velocities
$\bar{w}$	post-collisional angular velocity
y	packing fraction ($\pi\rho/6$)
Z	pressure equation of state (pV/NkT)

References

Alder B J and Wainwright T W 1960 *J. Chem. Phys.* **33** 1439–55

Barker G C 1993 Computer simulation of granular materials *Granular Matter* ed A Mehta (Berlin: Springer) ch 2

Bryan G H 1894 *Annual Report* British Association for the Advancement of Science **64** 83–4

Carnahan N E and Starling N E 1969 Equation of state for nonattracting rigid spheres *J. Chem. Phys.* **51** 635–6

Chapman S and Cowling T G 1970 *The Mathematical Theory of Non-uniform Gases* (Cambridge: Cambridge University Press)

Edwards S F 1993 The role of entropy in the specification of a powder *Granular Matter* ed A Mehta (Berlin: Springer) ch 4

Goldsmith W 1960 *Impact* (London: Edward Arnold)

Knight T A 1993 Computer studies of aerosols by hard-sphere granular dynamics *PhD Thesis* University of Bradford

Lun C K K and Savage S B 1987 A simple theory for granular flow of rough, inelastic spherical particles *J. Appl. Mech.* **54** 47–53

Pippard A B 1985 *Response and Stability. An Introduction to the Physical Theory* (Cambridge: Cambridge University Press)

Pidduck F B 1922 The kinetic theory of a special type of rigid molecule *Proc. R. Soc.* A **C11** 101–10

Turner M C and Woodcock L V 1990 Scaling Laws for Rapid Granular Flow *Powder Technology* **60** 47–60

Warr S, Huntley J M and Jaques G T H 1995a Fluidisation of a two-dimensional granular system: Experimental study and scaling behaviour *Phys. Rev.* E **52** 5583–95

Warr S and Huntley J M 1995b Energy input and scaling laws for a single particle vibrating in one dimension *Phys. Rev.* E **52** 5596–601

Woodcock L V 1981 Glass transition in the hard-sphere model and Kauzmann's Paradox *Ann. NY Acad. Sci.* **371** 274–98